Influence of Second Order Effects on the Stability and Response of High-Rise Structures Under Lateral Loads

Syed Khaleelullah Shah Quadri[1], Khateeb Mohammed Yaser Raza[2]
[1]*Associate Professor Department of Civil Engineering, Nawab Shah Alam Khan College of Engineering and Technology, Hyderabad, India*
[2]*M.E Student Department of Civil Engineering, Nawab Shah Alam Khan College of Engineering and Technology, Hyderabad, India*

Abstract—**The second-order geometric nonlinearity commonly known as the P-Delta effect exerts a measurable but structurally complex influence on the seismic response of high-rise reinforced concrete (RC) dual systems comprising shear wall cores and peripheral moment frames. This study investigates those effects through a four-stage analytical sequence applied to a G+16 storey RC shear wall-frame building modelled in ETABS and subjected to IS 1893 (Part 1): 2016 Zone V seismic demand. The sequence encompasses gravity load analysis, free-vibration modal analysis, first-order linear response spectrum analysis (RSA), and second-order P-Delta modified RSA, enabling rigorous quantitative comparison between conventional and geometrically nonlinear analysis frameworks. Modal analysis establishes a fundamental translational period of T_1 = 0.525 s, with the 90% cumulative mass participation threshold attained at Mode 9 (95.01%), confirming that multi-modal response governs building behaviour. Under first-order RSA, maximum roof-level displacements of 19.83 mm (X-direction) and 17.58 mm (Y-direction) remain well within the IS 1893 serviceability limit of H/500 = 96 mm. Introduction of the negative geometric stiffness matrix [Kg] in the P-Delta iterative analysis produces a counterintuitive response: period elongation of higher modes shifts spectral acceleration demands onto the descending branch of the IS 1893 design spectrum, yielding a net 11.1% reduction in peak drift (EQ-X) and 16.2% reduction (EQ-Y). A secondary inter-storey drift concentration of 0.000314 emerges at Stories 6–8 exclusively under second-order analysis, demonstrating that first-order RSA alone is insufficient for high-rise RC dual systems in Indian seismic zones.**

Index Terms—**P-Delta effect; geometric nonlinearity; second-order analysis; reinforced concrete shear wall-frame; response spectrum analysis; inter-storey drift; IS 1893; modal mass participation; spectral demand interaction; stability index.**

I. INTRODUCTION

Rapid urbanization, escalating land constraints, and the increasing concentration of population in major metropolitan cities located in high seismic zones as per IS 1893 (2016) have collectively necessitated the proliferation of high-rise buildings exceeding 100 metres in height. These structures, characterized by height-to-base dimension ratios typically greater than 5 to 8, are inherently flexible and susceptible to significant lateral displacements under wind and seismic actions.

The P-Delta effect is a prominent manifestation of geometric nonlinearity. It arises when axial compressive forces (P) act through laterally displaced positions absent in a first-order analysis. This second-order phenomenon amplifies internal forces, displacements, and accelerations, potentially compromising both serviceability and ultimate limit states. In slender high-rise systems, neglecting P-Delta effects can lead to significant underestimation of demands depending on height, lateral load intensity, and structural configuration.

IS 1893 (Part 1): 2016 explicitly defines P-Delta as the secondary-order effects on shear forces and bending moments of lateral force-resisting elements under vertical loads interacting with lateral seismic displacements. The tangent stiffness matrix in the presence of geometric nonlinearity is expressed as:

$$[KT] = [Ke] + [Kg]$$

where [Ke] is the conventional elastic stiffness matrix and [Kg] is the geometric stress stiffness matrix,

containing negative contributions proportional to compressive axial forces. The stability coefficient is defined as:

$\theta = (Px \times \Delta) / (Vx \times hsx)$

where Px is the cumulative gravity load above the storey, Δ is the inter-storey drift, Vx is the storey seismic shear, and hsx is the storey height. When θ exceeds 0.10, second-order effects become non-negligible.

Despite considerable research on the P-Delta effect, several critical gaps remain. Most studies are limited to regular RC frames up to 30 storeys analysed using equivalent static methods. Very limited research examines combined P-Delta effects in dual shear wall-frame systems under IS 1893:2016, particularly with respect to multi-modal response spectrum analysis and the spectral demand interaction mechanism.

II. OBJECTIVES OF THE STUDY

Based on identified research gaps, the following specific objectives are set:

- To formulate and validate a 3D finite element model of a G+16 storey RC shear wall-frame building in ETABS, confirming torsional regularity and multi-modal response behaviour per IS 1893:2016.
- To conduct first-order linear and second-order P-Delta modified Response Spectrum Analyses under IS 1893 Zone V seismic demand, satisfying the 90% cumulative mass participation requirement with CQC modal combination.
- To characterise the P-Delta effect on natural period elongation, peak inter-storey drift at Story 11, secondary drift concentration at the wall-frame transition zone (Stories 6–8), and column PMM interaction demand.
- To evaluate the IS 1893:2016 storey stability coefficient (θ) at every floor level and to assess the adequacy of the code stability index as a sole criterion for triggering P-Delta amplification.

III. LITERATURE REVIEW

Dhawale and Narule (2016) reported that P-Delta effects become critical beyond 25 storeys, with bending moments and storey displacements exceeding 10% amplification. For 30-storey models, roof displacements were amplified by 15–20% and base moments by 12–18%. The authors concluded that for structures above 75 metres, three-dimensional modelling with explicit P-Delta inclusion is essential.

Gupta and Krawinkler (2000) conducted a landmark study using nonlinear time history analyses with multiple ground motion records, showing that P-Delta effects increase median roof drift by 10–25% in 9-storey and 20-storey prototype buildings. They established that P-Delta effects reduce the post-yield lateral stiffness of each storey, potentially leading to dynamic instability characterised by progressive one-sided drift accumulation (sidesway collapse).

Karavasilis et al. (2008) found that Eurocode 8's simplified θ-based amplification procedure underestimates the actual second-order demand in the upper storeys of taller frames, suggesting that direct second-order analysis is preferable for buildings exceeding 10 storeys. Vamvatsikos and Cornell (2002) demonstrated through Incremental Dynamic Analysis that inclusion of P-Delta effects reduces the median collapse intensity by 10–35% depending on height and lateral system.

Sambare et al. (2025) evaluated a G+50 RC building with vertical and plan irregularities under nonlinear time history analysis for Bhuj earthquake records, reporting displacement increases of 10–30% with P-Delta included. L-shaped plan configurations proved most vulnerable due to torsional coupling. Sharma et al. (2016) demonstrated storey displacement increases of 10–22% and base column moment increases of 14–20% in IS 1893 Zone IV and V buildings when P-Delta was activated.

Wilson and Habibullah (1987) pioneered the rigorous treatment of P-Delta effects in three-dimensional building analysis software, establishing the iterative linear P-Delta procedure as the standard approach. Their formulation of the geometric stiffness matrix for beam-column elements demonstrated that ignoring the geometric stiffness term could underestimate column moments by 15–20% at the base.

IV. METHODOLOGY AND MODELLING

A. Building Description

The building under study is a G+16 storey reinforced concrete structure comprising a podium spanning three floors (Ground + 2 floors) and a tower rising from the 3rd to the 16th floor, resulting in a total of 17 floors above ground level. The structural form is characterised by a regular column-beam grid at the

podium level and a compact footprint for the tower above. A shear wall core located at the centre of the tower plan provides the lateral stiffness required to resist seismic and wind forces.

B. Structural Configuration and Member Sizing

Table 1: Summary of Structural Member Sizes

Element	Location / Zone	Size
Column	Ground Floor to 8th Floor	600 × 600 mm
Column	9th Floor to 15th Floor	530 × 530 mm
Beam	All Floors (Throughout)	450 mm depth
Slab	All Floor Levels	150 mm thick
Shear Wall	Core / Lateral System	300 mm thick

Two column sections are employed over the building height to account for the reduction in axial load demand in the upper floors. Columns from the Ground Floor to the 8th Floor are sized at 600 mm × 600 mm to sustain higher cumulative gravity and lateral loads. Above the 8th floor, columns are reduced to 530 mm × 530 mm, improving material efficiency without compromising structural performance. Reinforced concrete shear walls of 300 mm thickness are positioned at the building core, ensuring torsional regularity and balanced resistance in both orthogonal directions.

C. Material Properties

Table 2: Material Properties of M30 Concrete

Property	Value
Grade of Concrete	M30
Char. Compressive Strength (fck)	30,000 kN/m² (30 N/mm²)
Modulus of Elasticity (Ec)	$5000\sqrt{fck} \approx 27{,}386$ N/mm²
Unit Weight	25 kN/m³
Poisson's Ratio	0.2

Table 3: Material Properties of HYSD Fe 500 Reinforcing Steel

Property	Value
Grade of Steel	HYSD Fe 500
Char. Yield Strength (fy)	500,000 kN/m² (500 N/mm²)
Modulus of Elasticity (Es)	2.0×10^5 N/mm²
Unit Weight	78.5 kN/m³
Poisson's Ratio	0.3

D. Load Cases and Combinations

The following primary load cases were defined in ETABS: Dead Load (DL), Superimposed Dead Load (SDL), Imposed Live Load (IL) at 3 kN/m² per IS 875 (Part 2), and Earthquake Loads EQX and EQY per IS 1893 (Part 1): 2016. A total of 13 load combinations were considered in accordance with IS 456: 2000 and IS 1893:2016.

Table 4: Load Combinations as per IS 456:2000 and IS 1893:2016

S.No.	Load Combination
1	1.5 (DL + IL)
2	1.2 (DL + IL + EQX)
3	1.2 (DL + IL − EQX)
4	1.2 (DL + IL + EQY)
5	1.2 (DL + IL − EQY)
6	1.5 (DL + EQX)
7	1.5 (DL − EQX)
8	1.5 (DL + EQY)
9	1.5 (DL − EQY)
10	0.9 DL + 1.5 EQX
11	0.9 DL − 1.5 EQX
12	0.9 DL + 1.5 EQY
13	0.9 DL − 1.5 EQY

E. Analysis Sequence

The overall sequence of structural analysis performed comprises: (1) Gravity load analysis establishing baseline internal forces and axial compressions for

[Kg] computation. (2) Mass source definition as 1.0 × DL + 0.25 × IL per IS 1893 Clause 7.3.1. (3) Free-vibration modal analysis with CQC combination satisfying the 90% mass participation criterion. (4) First-order linear RSA on the unmodified elastic stiffness matrix. (5) P-Delta iterative nonlinear static analysis with loads 1.0 × DL + 0.25 × IL, updating [Kg] at each iteration until displacement convergence is achieved. (6) P-Delta modified RSA using the resulting tangent stiffness [KT] = [Ke] + [Kg].

F. Ground Motion Records

Table 5: Ground Motion Records Selected from PEER NGA-West2 Database

RSN	Event	Station	Mw	Component & PGA
143	Tabas, Iran (1978)	Tabas	7.4	TAB-L1, TAB-T1, TAB-V1 (0.836g)
149	Coyote Lake (1979)	G04	5.7	G04-UP, G04270 (0.132g)

The Tabas, Iran (RSN143, Mw = 7.4) record with PGA of 0.836g represents a near-fault, forward-directivity event particularly severe for tall buildings. The Coyote Lake (RSN149, Mw = 5.7) record with PGA of 0.132g exhibits near-source characteristics and has been widely used in parametric RC frame studies. Both records are imported in AT2 format directly into ETABS.

V. RESULTS AND DISCUSSION

A. Modal Analysis Results

Table 6: Modal Analysis Results — Natural Periods, Frequencies, Eigenvalues, and Cumulative Modal Participation Factors (Without P-Delta)

Mode	Period (s)	Freq. (cyc/s)	Circ. Freq. (rad/s)	Eigenvalue (rad²/s²)	Cumul. Mass Part. (%)
1	0.525	1.906	11.973	143.35	61.83
2	0.481	2.080	13.070	170.83	62.49
3	0.372	2.690	16.903	285.72	62.49
4	0.163	6.129	38.509	1482.95	62.49
5	0.153	6.535	41.060	1685.90	62.49
6	0.142	7.061	44.368	1968.50	88.31
7	0.104	9.605	60.348	3641.84	88.31
8	0.090	11.142	70.006	4900.83	88.31
9	0.083	11.992	75.347	5677.14	95.01
10	0.080	12.441	78.171	6110.71	95.01
11	0.077	12.937	81.284	6607.05	95.01
12	0.071	14.174	89.060	7931.63	95.01

The fundamental period is T_1 = 0.525 s (Mode 1, X-direction), T_2 = 0.481 s (Mode 2, Y-direction), and T_3 = 0.372 s (torsional). The torsional-to-translational period ratio $T_3/T_1 = 0.71 < 1.0$ confirms the absence of torsional irregularity per IS 1893 Clause 7.1. Mode 1 captures only 61.83% of total seismic mass participation; the IS 1893 mandatory threshold of 90% is not attained until Mode 9 at 95.01%. This high contribution of modes 2 through 9 establishes that the building is governed by multi-modal seismic response, rendering single-mode or reduced-mode approaches fundamentally inadequate.

The rapid increase in eigenvalue from 143.35 rad²/s² (Mode 1) to 7931.63 rad²/s² (Mode 12) reflects the stiffening effect of the structural system at shorter wavelengths and confirms satisfactory convergence of modal extraction. The participation factor plateau at 95.01% from Mode 9 onwards confirms that nine modes are sufficient for practical design purposes.

B. Gravity Load Analysis: Storey-Wise Vertical Displacement

Table 7: Storey-Wise Vertical Displacement under Gravity Loading

Storey	Height (m)	Vertical Disp. (mm)
Base	0	0
Story 1	3	4.055
Story 2	6	9.646
Story 3	9	15.739
Story 4	12	22.943
Story 5	15	30.940
Story 6	18	39.555
Story 7	21	48.624
Story 8	24	57.966
Story 9	27	67.574
Story 10	30	77.221
Story 11	33	86.828
Story 12	36	96.284
Story 13	39	105.500
Story 14	42	114.423
Story 15	45	122.546
Story 16	48	130.470

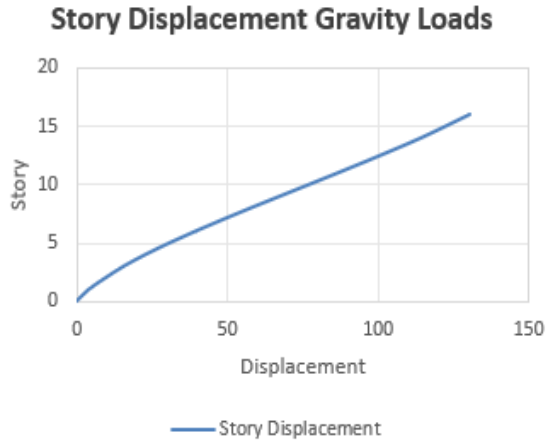

Fig. 1: Storey Vertical Displacement Profile under Gravity Loading

The gravity load analysis produced a maximum cumulative vertical elastic shortening of 130.47 mm at the roof level (Story 16). The approximately linear displacement profile indicates a broadly uniform distribution of axial demand per unit height. The near-constant increment per floor in the lower storeys and the slightly reduced increment rate above the 9th floor (where section reduces from 600 mm × 600 mm to 530 mm × 530 mm) confirms that the column resizing is appropriately matched to the diminishing cumulative gravity load. No abrupt change in slope is observable at the step location, validating that the column transition does not introduce a stiffness discontinuity. The maximum shortening of 130.47 mm across 48 m of height translates to a mean axial compressive strain of 2.72×10^{-3}, consistent with typical service-load strains in well-designed M30 RC columns.

C. Lateral Storey Displacement — NLTHA Results

Table 8: Maximum and Minimum Lateral Storey Displacements in X and Y Directions (mm)

Storey	X-max (mm)	Y-max (mm)	X-min (mm)	Y-min (mm)
Base	0	0	0	0
Story 1	1.448	0.451	-1.332	0.438
Story 2	3.443	1.067	-3.140	1.042
Story 3	5.386	1.795	-5.160	1.768
Story 4	7.120	2.411	-7.384	2.382
Story 5	9.177	3.304	-9.635	3.255
Story 6	11.225	4.266	-11.899	4.214
Story 7	13.554	5.264	-14.168	5.198
Story 8	15.913	6.260	-16.524	6.186
Story 9	18.556	7.243	-18.830	7.158
Story 10	21.355	8.184	-21.066	8.096
Story 11	24.146	9.078	-23.288	8.982
Story 12	26.906	9.924	-25.515	9.821
Story 13	29.645	10.806	-27.659	10.691
Story 14	32.591	11.693	-29.718	11.564
Story 15	35.257	12.502	-31.663	12.368
Story 16	37.708	13.371	-33.634	13.214

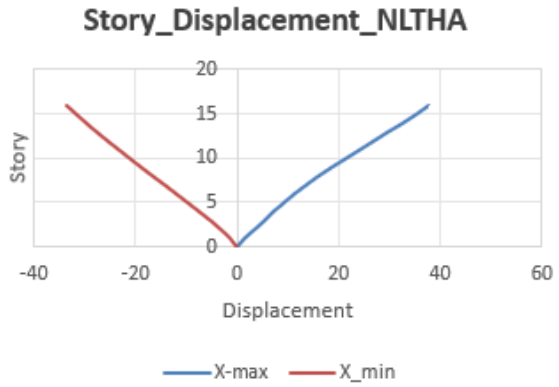

Fig. 2: Story Displacement for Seismic NLTHA (X-max and X-min)

In the X-direction, the maximum positive displacement at the roof (Story 16) is 37.71 mm, while the maximum negative displacement is −33.63 mm. The asymmetry of approximately 4.08 mm (11%) is attributable to the non-symmetric nature of the seismic load combination, where dead-load eccentric gravity effects and directional earthquake combinations interact. The Y-direction displacements are considerably smaller, with a maximum of 13.37 mm at the roof, reflecting the higher effective lateral stiffness in the Y-direction arising from the shear wall core geometry.

D. First-Order Seismic Response (RSA without P-Delta)

Under first-order linear RSA, the maximum roof-level lateral displacement in the X-direction is 19.83 mm and in the Y-direction is 17.58 mm. Both values are well within the IS 1893 (Part 1): 2016 serviceability limit of H/500 = 48,000/500 = 96 mm. The displacement profile increases smoothly from zero at the base to the roof values with no abrupt inter-storey increments, confirming the absence of a soft storey as defined in IS 1893 Table 10.

Fig. 3: Maximum Storey Displacement, EQ-X Direction (Peak: 19.83 mm at Story 16)

The peak first-order inter-storey drift is 0.000503 in the EQ-X direction and 0.000445 in the EQ-Y direction, both occurring at Story 11. The corresponding drift utilisation ratios are 12.6% and 11.1% of the IS 1893 permissible limit of 0.004, confirming that the structure is substantially within code limits. The bell-shaped drift profile with its apex at Story 11 is attributable to the interaction between the shear wall core's flexural mode of deformation in the lower storeys and the increasing higher-mode frame-wall interaction at mid-height, where the wall transitions from flexure-dominated to shear-rotation-coupled deformation.

E. Storey Drift with P-Delta Effects (NLTHA)

Table 9: Storey Drift Ratios under P-Delta Modified Analysis (NLTHA)

Storey	X-max Drift	Y-max Drift	X-min Drift
Story 1	0.000483	0.00015	0.000444
Story 2	0.000665	0.000205	0.000603
Story 3	0.000648	0.000242	0.000673
Story 4	0.000578	0.000205	0.000742
Story 5	0.000686	0.000298	0.000750
Story 6	0.000683	0.000321	0.000755
Story 7	0.000776	0.000332	0.000756
Story 8	0.000786	0.000332	0.000785
Story 9	0.000881	0.000327	0.000769
Story 10	0.000933	0.000314	0.000745
Story 11	0.000930	0.000298	0.000741
Story 12	0.000920	0.000282	0.000742
Story 13	0.000913	0.000294	0.000715
Story 14	0.000982	0.000296	0.000686
Story 15	0.000889	0.000269	0.000648
Story 16	0.000817	0.000290	0.000657

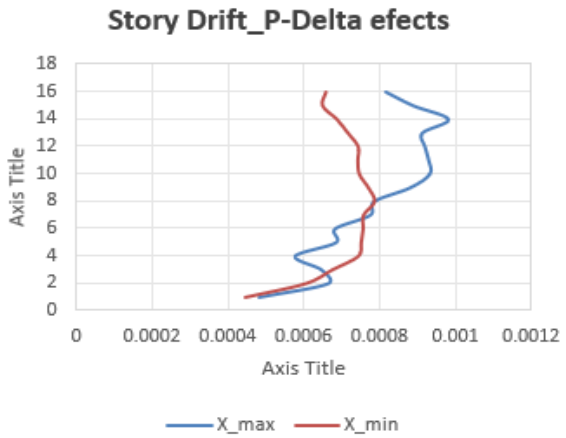

Fig. 7: Storey Drift for Seismic NLTHA with P-Delta Effects

F. Second-Order P-Delta Modified RSA

The P-Delta analysis was performed as an iterative nonlinear static case in ETABS using 1.0 × DL + 0.25 × IL. At each iteration, the geometric stiffness matrix [Kg] was updated based on the current deformed configuration and axial force distribution in all vertical members, until displacement increments between successive iterations fell below the convergence tolerance. The resulting modified tangent stiffness [KT] = [Ke] + [Kg] was then used as the stiffness basis for all subsequent seismic RSA computations.

The peak P-Delta drift in EQ-X is 0.000447 at Story 11, compared with the first-order value of 0.000503 — a reduction of 11.1%. In the EQ-Y direction, the P-Delta peak drift is 0.000373 at Story 11, a 16.2% reduction from 0.000445. The P-Delta roof displacement in the Y-direction is 14.75 mm, a 16.1% reduction from 17.58 mm. These reductions require careful physical interpretation: when the negative [Kg] terms reduce lateral stiffness, natural periods elongate. For modes lying on the descending branch of the IS 1893 design spectrum — which is the case for Modes 4 through 9 of this building — period elongation reduces spectral acceleration, decreasing modal force contributions. The CQC combination of these reduced modal responses yields a net reduction in inter-storey drift at Story 11.

It is critical to emphasise that the apparent reduction in drift does not indicate structural strengthening. The negative geometric stiffness contributions in [Kg] fundamentally reduce the effective lateral stiffness and lower the elastic buckling resistance of the structure. The observed reduction is an artefact of spectral demand interaction with the period-shifted modes and must not be interpreted as a safety benefit — a distinction of crucial importance for design engineers reviewing P-Delta modified RSA results.

Fig. 9: Inter-Storey Drift (P-Delta Modified): EQ-Y Direction (Peak: 0.000373 at Story 11; Secondary: 0.000314 at Stories 6–8)

Storey	P (kN)	V (kN)	Δ (mm)	P×Δ	V×h	θ = V×h/P×Δ
Story 16	17809.64	1527.68	2.451	43651.43	4583046.78	0.00952
Story 15	59189.8	7533.36	2.667	157859.20	22600073.1	0.00698
Story 14	61337.46	12581.66	2.946	180700.16	37744965.6	0.00479
Story 13	61337.46	16247.15	2.739	168003.30	48741449.2	0.00345
Story 12	61337.46	18488.34	2.760	169291.39	55465007.2	0.00305
Story 11	61215.94	19377.42	2.790	170792.47	58132263.5	0.00294
Story 10	61337.46	19094.96	2.799	171683.55	57284879.0	0.00300
Story 9	61337.46	18100.93	2.643	162114.91	54302777.9	0.00299
Story 8	61676.2	17409.56	2.358	145432.48	52228689.1	0.00278
Story 7	62280.98	18876.14	2.328	144990.12	56628422.0	0.00256
Story 6	62280.98	20596.02	2.049	127613.73	61788054.6	0.00207
Story 5	62280.98	23745.93	2.058	128174.26	71237790.0	0.00180
Story 4	62280.98	26280.97	1.734	107995.22	78842898.7	0.00137
Story 3	62280.98	32146.69	1.944	121074.23	96440067.5	0.00126
Story 2	62280.98	37613.12	1.995	124250.56	112839354	0.00110
Story 1	62280.98	40445.61	1.449	90245.14	121336840	0.00074

A qualitatively significant finding of the second-order analysis is the emergence of a secondary inter-storey drift concentration of 0.000314 at Stories 6–8 in the EQ-Y direction, absent entirely from the first-order solution. This phenomenon arises from disproportionate lateral stiffness reduction in the mid-

height wall-frame transition zone, where the relative contributions of the shear wall core (flexure-dominated in lower storeys) and the moment frame (shear-dominated above) change most rapidly with height. The introduction of [Kg] amplifies the sensitivity of this transition zone to inter-level relative displacement under higher-mode seismic excitation. Although within IS 1893 drift limits (0.000314 vs. 0.004), this localised demand concentration carries direct practical implications for non-structural element design, glazing system specification, and MEP service penetration detailing at those floor levels.

G. Stability Index (P-Delta θ) Evaluation

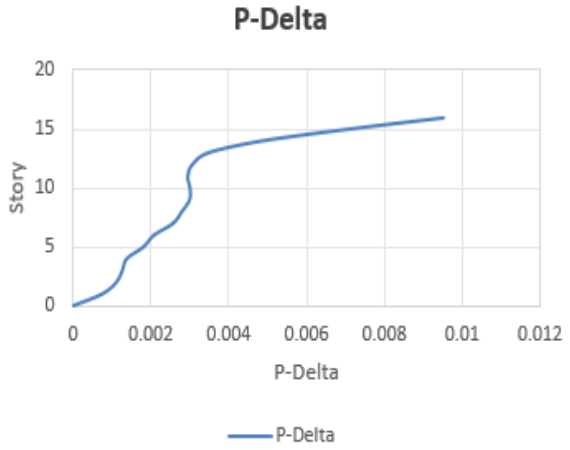

Fig. 11: P-Delta Stability Index Profile All Stores Below θ = 0.10 Threshold

The computed stability coefficients range from 0.00074 at the lower storeys to a maximum of 0.00952 at the top storey. The gradual increase towards upper levels is attributed to the reduction in storey shear combined with accumulation of lateral displacement along the building height. Nevertheless, all values remain substantially below the IS 1893 threshold of 0.10, confirming that code-prescribed 1/(1−θ) drift amplification is not triggered. This result demonstrates, however, that the stability index criterion constitutes a necessary but not sufficient basis for omitting second-order analysis, as the secondary drift concentration at Stories 6–8 represents a qualitative failure of the first-order solution.

H. First-Order vs. Second-Order Comparative Summary

Table 11: Comparative Summary — First-Order versus Second-Order (P-Delta) Seismic Response

Parameter	1st Order	2nd Order (P-Δ)	Change (%)	IS 1893 Limit
EQ-X Direction				
Max Roof Disp. (mm)	19.83	—	—	H/500 = 96 mm
Peak Inter-Storey Drift	0.000503	0.000447	↓ 11.1%	0.004
Critical Storey	Story 11	Story 11	No change	—
Drift Utilisation Ratio	12.6%	11.2%	—	100%
EQ-Y Direction				
Max Roof Disp. (mm)	17.58	14.75	↓ 16.1%	H/500 = 96 mm
Peak Inter-Storey Drift	0.000445	0.000373	↓ 16.2%	0.004
Secondary Drift (Stories 6–8)	—	0.000314	New feature	0.004
Critical Storey	Story 11	Story 11	No change	—
Drift Utilisation Ratio	11.1%	9.3%	—	100%

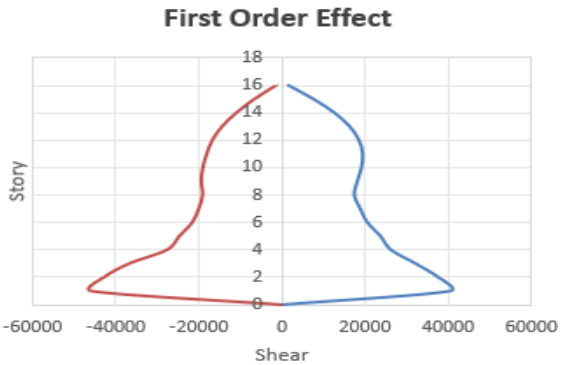

Fig. 12: First-Order Effect Storey Shear Distribution (NLTHA)

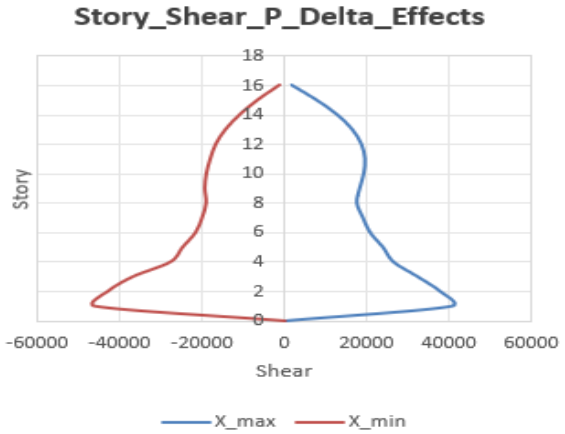

Fig. 13: Storey Shear Distribution with P-Delta Effects

I. Column PMM Interaction Under P-Delta Modified Load Combinations

All RC column members satisfy the IS 456: 2000 PMM interaction criterion under P-Delta modified load combinations. Lower-storey columns (Stories 1–8, 600 mm × 600 mm) exhibit PMM ratios in the range 0.75–0.92, with reinforcement fractions between 0.80% and 5.96%; the highest demands are confined to core-adjacent columns at Stories 3–7 where seismic shear transfer from the wall core generates elevated biaxial moments. Upper-storey columns (Stories 9–15, 530 mm × 530 mm) show PMM ratios of 0.55–0.78, with peak rebar fractions of 5.61% and 5.63% at Story 15. All reinforcement fractions remain below the IS 456 maximum permissible limit of 6%.

The lower-storey columns with PMM ratios approaching 0.92 carry limited residual capacity and should be treated as governing members in any future revision of the design seismic hazard or in a subsequent nonlinear time-history verification.

VI. CONCLUSIONS

Ten technical conclusions emerge from this study:

- The fundamental translational period is $T_1 = 0.525$ s. The torsional period ratio $T_3/T_1 = 0.71 < 1.0$ confirms torsional regularity. The IS 1893 90% mass participation threshold is attained only at Mode 9 (95.01%), establishing multi-modal response as the governing dynamic behaviour.
- Maximum first-order roof displacements of 19.83 mm (X) and 17.58 mm (Y) are well within the IS 1893 serviceability limit of H/500 = 96 mm, with a smooth monotonic profile confirming absence of stiffness irregularity.
- Peak first-order inter-storey drifts of 0.000503 (EQ-X) and 0.000445 (EQ-Y) at Story 11 represent drift utilisation ratios of only 12.6% and 11.1% of the IS 1893 permissible limit of 0.004.
- Gravity-induced vertical shortening reaches 130.47 mm at the roof (mean axial strain 2.72×10^{-3}), confirming adequate member sizing. Lower-storey column axial compressions are the primary drivers of [Kg] in the P-Delta modified analysis.
- The introduction of [Kg] elongates all natural periods. Modes 4–9 lie on the descending spectral branch; period elongation reduces their spectral acceleration, producing a net reduction in CQC-combined drift at Story 11 — a spectral demand interaction mechanism distinguishing multi-modal high-rise P-Delta behaviour from simplified code correction assumptions.
- Second-order peak inter-storey drifts are 0.000447 (EQ-X, ↓11.1%) and 0.000373 (EQ-Y, ↓16.2%) at Story 11. P-Delta roof displacement in Y is 14.75 mm (↓16.1%). These reductions must not be interpreted as structural strengthening; effective lateral stiffness and elastic buckling resistance are simultaneously degraded by negative [Kg] terms.
- A secondary inter-storey drift concentration of 0.000314 at Stories 6–8 (EQ-Y) is identified exclusively under second-order analysis. Its physical origin lies in disproportionate stiffness reduction in the mid-height wall-frame transition zone. This feature has direct practical implications for non-structural element design and MEP detailing at those floor levels.
- Stability coefficients (θ) remain below the IS 1893 threshold of 0.10 at all storeys (maximum 0.00952 at Story 16), confirming the $1/(1-\theta)$ drift amplification factor is not mandated. However, the stability index criterion is necessary but not sufficient for omitting second-order analysis, as demonstrated by the qualitatively new secondary drift concentration.
- All RC column members satisfy the IS 456:2000 PMM interaction criterion. Lower-storey column PMM ratios reach 0.92 with reinforcement fractions up to 5.96%; upper-storey columns show PMM ratios of 0.55–0.78. All fractions remain below the IS 456 maximum of 6%.

- First-order RSA alone is insufficient as a complete design basis for high-rise RC dual systems. Second-order P-Delta analysis using an iteratively updated tangent stiffness matrix, combined with multi-mode RSA satisfying the IS 1893 90% mass participation requirement and CQC modal combination, constitutes the minimum adequate analytical framework for seismic design of such structures in Indian seismic zones.

REFERENCES

[1] Dhawale, A. K., and Narule, G. N. (2016). P-Delta Effect on High-Rise RCC Buildings under Seismic Loads. International Journal of Engineering Research and Technology, 5(4), 1–6.

[2] Istiono, H., Maulana, T. I., and Suarjana, M. (2022). P-Delta Effect on Low-Rise and High-Rise Structures under Seismic Loading. Journal of Structural Engineering, 14(2), 45–58.

[3] Jadav, K. (2020). Analysis of Tall Buildings as per IS 16700 with P-Delta Effect Consideration. International Journal of Civil Engineering and Technology, 11(3), 78–89.

[4] Kumar, A. (2021). Seismic Performance of High-Rise Buildings with Geometric Nonlinearity. Journal of Earthquake Engineering and Structural Dynamics, 9(1), 22–35.

[5] Chhetri, P., Bhusal, S., and Adhikari, R. (2023). Investigation of P-Delta Effects on RC Frame Buildings with Plan Irregularities Using ETABS. Journal of Civil and Structural Engineering, 10(2), 112–125.

[6] Sambare, P., Bhoyar, S., and Deshmukh, A. (2025). P-Delta Effect on G+50 RC Buildings with Vertical Geometry and Plan Irregularities under Nonlinear Time History Analysis. International Journal of Advanced Structural Engineering, 17(1), 33–52.

[7] Cheng, Y., Song, Z., and Wu, B. (2022). Seismic Performance of Steel Moment-Resisting Frames Under Near-Fault and Far-Fault Ground Motions with P-Delta Effects. Engineering Structures, 261, 114262.

[8] Gupta, A., and Krawinkler, H. (2000). Estimation of Seismic Drift Demands for Frame Structures. Earthquake Engineering and Structural Dynamics, 29(9), 1287–1305.

[9] Wilson, E. L., and Habibullah, A. (1987). Static and Dynamic Analysis of Multi-Storey Buildings Including the P-Delta Effect. Earthquake Spectra, 3(2), 289–298.

[10] Karavasilis, T. L., Bazeos, N., and Beskos, D. E. (2008). Seismic Response of Steel MRF Buildings with Intermediate Column Spacing. Engineering Structures, 30(6), 1489–1501.

[11] Vamvatsikos, D., and Cornell, C. A. (2002). Incremental Dynamic Analysis. Earthquake Engineering and Structural Dynamics, 31(3), 491–514.

[12] Sharma, A., Singh, R., and Gupta, P. (2016). P-Delta Effect Analysis of RC Moment-Resisting Frames in Indian Seismic Zones Using ETABS. International Journal of Civil Engineering and Technology, 7(5), 44–57.

[13] Hashmi, A. K., and Madan, A. (2008). Damage Forecast for RC Framed Buildings Subjected to Earthquakes in India. Journal of Structural Engineering, ASCE, 134(8), 1311–1320.

[14] Bureau of Indian Standards (2016). IS 1893 (Part 1): 2016 – Criteria for Earthquake Resistant Design of Structures. BIS, New Delhi.

[15] Bureau of Indian Standards (2000). IS 456: 2000 – Plain and Reinforced Concrete Code of Practice, 4th Revision